




Article

Traditional and Modern Plasters for Built Heritage: Suitability and Contribution for Passive Relative Humidity Regulation

Alessandra Ranesi ^{1,2,*} , Paulina Faria ¹  and Maria do Rosário Veiga ² 

¹ CERIS and Department Civil Engineering, NOVA School of Science and Technology, NOVA University of Lisbon, 2829-516 Caparica, Portugal; paulina.faria@fct.unl.pt

² National Laboratory for Civil Engineering, Avenida do Brasil 101, 1700-066 Lisbon, Portugal; rveiga@lnec.pt

* Correspondence: a.ranesi@campus.fct.unl.pt

Abstract: Plasters have covered wide surface areas of buildings since antiquity, with a main purpose of indoor protection of the substrate on which they are applied. When no longer functional, they might require substitution with solutions that can combine compatibility with the substrate with the current need to mitigate building emissions. Indeed, plasters can contribute to lowering buildings' energy demands while improving indoor air quality and the comfort of buildings' users, as plasters can be used as passive regulators of relative humidity (RH). Hence, this study presents the relative-humidity-dependent properties of different plastering mortars based on clay, air lime, and natural hydraulic lime, and plastering finishing pastes based on gypsum and gypsum–air lime, in all cases tested using small size specimens. A cement-based plaster is also analysed for comparison. The clay-based plaster was the most promising material for RH passive regulation, and could be applied to repair and replace plasters in different types of buildings. Pastes based on air lime–gypsum could be applied as finishing layers, specifically on traditional porous walls. The sorption behaviour of cement plaster appeared interesting; however, its water vapour permeability was as expected, found to be the lowest, discouraging its application on historic walls.

Keywords: air lime; clay; gypsum; hygroscopicity; moisture passive regulation; mortar; natural hydraulic lime; paste; plaster; water vapour permeability



Citation: Ranesi, A.; Faria, P.; Veiga, M.d.R. Traditional and Modern Plasters for Built Heritage: Suitability and Contribution for Passive Relative Humidity Regulation. *Heritage* **2021**, *4*, 2337–2355. <https://doi.org/10.3390/heritage4030132>

Academic Editors: John J. Hughes, Alexandre S. Gagnon and Elena Sesana

Received: 29 July 2021

Accepted: 7 September 2021

Published: 10 September 2021

Publisher's Note: MDPI stays neutral with regard to jurisdictional claims in published maps and institutional affiliations.



Copyright: © 2021 by the authors. Licensee MDPI, Basel, Switzerland. This article is an open access article distributed under the terms and conditions of the Creative Commons Attribution (CC BY) license (<https://creativecommons.org/licenses/by/4.0/>).

1. Introduction

Plasters are “a mix of one or more binders, sand, water and sometimes additives” [1] that have been used for covering interior walls and ceilings since antiquity. Thus, traditional plasters cover a large surface of historical buildings and represent themselves as part of the built heritage. The old plasters were commonly based on clayey earth, air lime, and gypsum [2,3]. Only in the late 19th century did those materials begin to be replaced with hydraulic binders, such as hydraulic lime, natural cement, and Portland cement [4]. Thus, during the 20th century, many interventions oriented to the repair and conservation of old buildings were carried out with complete substitution of original mortars with new binder-based ones [5], which frequently contributed to accelerating the degradation process of the built heritage.

The main role of plasters is to protect the substrate on which they are applied, but they also serve improve living conditions. Nowadays, aspects related to respecting the eco-efficiency of interventions are also demanded. Hence, the intervention in historical buildings must consider compatibility criteria; i.e., physical, chemical, and mechanical compatibility [6], but also should aim to improve indoor air quality and decrease the energy demand of buildings. The passive regulation of relative humidity (RH) performed by plasters [7–9] has been largely discussed during the present century, since the interest in human health [10], indoor air quality (IAQ) [11], and perceived air quality [12] has spread, together with the aim of adapting historical buildings to climate change [13]. Moreover, the optimization of passive RH regulation represents an opportunity for improving indoor

comfort while reducing the need for HVAC systems, thus improving energy efficiency in historic buildings [14,15] and lowering their environmental impact and operational costs, which are fundamental to mitigate climate change [16] and reach a climate-neutral Europe by 2050 [17].

The assessment of the hygroscopic behaviour of plasters depends on some intrinsic properties of the plasters such as bulk density, pore size distribution, and porosity, combined with others such as the surface texture (partially related to application), as well as some properties that can be quantified only as a function of the RH fluctuation. To better understand the response of plasters when exposed to a change in hygrothermal conditions for a given period, the present study tested the RH-dependent properties of eight different plastering mortars and pastes based on traditional binders and newer hydraulic ones.

It is well known that cement-based plasters present low compatibility with built heritage due to their high mechanical resistance, low capillarity, low water vapour permeability, and high soluble salt content [18,19]. Moreover, while many studies have been conducted on the contribution that innovative plasters might provide to occupants' health and comfort, the same has been rarely assessed for traditional ones. Thus, the aim of this study was to characterize and quantify the response to RH variations of mortars and pastes based on traditional and contemporary binders, in order to assess compatibility and define possibilities of RH passive regulation.

2. Materials and Methods

2.1. Materials and Fresh State Characterization

In order to assess RH-dependent properties of a wide variety of plasters, one clay-based plaster specifically produced for this study [20] was tested together with seven different mortars and pastes that resulted from previous experimental campaigns [21–24]. The characterization of the clay-based plaster is presented and compared with the other plasters as described by their authors. Hence, the mortars and pastes included in the study were:

- A commercially available earthen plastering mortar (*E*) composed of clayish earth, mixed-grade sand of 0–2 mm, and barley straw fibers cut to less than 30 mm [20] mechanically mixed in the laboratory with addition of 20% by mass of water, as recommended by the producer (Embarro).
- Three pastes (not containing sand) designed as finishing restoration products [21] for old Portuguese interior finishings based on powder hydrated lime CL90-S (*CL*) and calcium sulphate hemihydrate–gypsum (*G*): *CL70_G20*, *CL50_G50*, and *G*. The *CL70_G20* was formulated using 70% hydrated lime, 20% gypsum, and 10% calcitic aggregate (<45 µm), with an addition of 0.1% of a water-retaining methylcellulose-based agent and 0.02% of a set retarder to assess the required workability. The same retarder in the same proportions was added to *CL50_G50* (50% hydrated lime and 50% gypsum), designed to mould on-site elements for gypsum plaster decoration. *G* was produced for restoration of precast elements with 100% of calcium sulphate hemi-hydrate. All the percentages are by mass.
- One plastering mortar made of hydrated lime (*CL*) and one made of natural hydraulic lime 3.5 (*NHL*), both mixed with siliceous sand from the Tagus River (0–4 mm) with a volumetric ratio of 1:3, corresponding to 1:13 and 1:6.7 by mass, respectively [22].
- Two cement plastering mortars [23,24] produced with CEM II/B-L 32.5 N and siliceous sand from the Tagus River (0–2 mm) with a volumetric ratio of 1:4, corresponding to 1:6 (*C_1.3*) and 1:5 (*C_0.9*) by mass.

The fresh characterizations of the earthen mortar and of all the other mortars and pastes, as reported by each author [21–24], are summarized in Table 1.

Table 1. Synthesis of fresh characterizations of selected plastering mortars and pastes.

Pastes and Mortars	Ref.	Month-Year of Production	Binder	Aggregate	b/a Ratio	w/b Ratio	Flow (mm)	BD (kg/dm ³)
G	[21]	04-2012	G (100%)	—	—	0.7	190 ± 5	nf
CL50_G50	[21]	03-2012	G (50%) CL (50%)	—	—	0.8	165 ± 5	nf
CL70_G20	[21]	03-2012	G (20%) CL (70%)	CA (10%)	—	1.0	165 ± 5	nf
E	—	02-2020	IE	SS02	nf	0.2	171 ± 10	1.95
CL	[22]	03-2016	CL 90-S	TR04	1:3	2.8	151 ± 5	nf
NHL *	—	03-2016	NHL 3.5	TR04	1:3	1.4	150 ± 5	nf
C_0.9	[23]	10-2018	CEM II/B-L 32.5N	SS02	1:4	0.9	140 ± 3	2.00
C_1.3	[24]	07-2017	CEM II/B-L 32.5N	SS02	1:4	1.3	161 ± 1	1.97

Notation: b/a—binder/aggregate; w/b—water/binder; Flow—flow table consistency; BD—wet bulk density; G—hemihydrate gypsum; CL—calcitic hydrated air lime; CA—fine calcitic aggregate; IE—illitic clay earth; SS02—natural siliceous sand (0–2 mm); TR04—Tagus River sand (0–4 mm); nf—not found; *—unpublished result; —water/mix ratio; ±—values for standard deviation. The % values are by mass.

The amount of mixing water was determined by each author in order to ensure the good workability of the mortar. The water content defined by the producer and used for the E plaster showed a flow within the limits of DIN 18947 [25] for earth plasters. The plaster/water ratio of the gypsum paste (G) was determined according to EN 13279-2 [26], while for lime–gypsum pastes (CL_Gs) and all the mortars, the flow table consistency method [27] was used [21]. Santos [22] stated that the amount of water added to CL and NHL mortars was quantified to ensure a flow table consistency of 150 ± 5 mm [27]. The flow table consistency was fixed at 140 ± 2 mm for C_0.9, which was quite a low value for cement plasters, and 165 ± 5 mm for C_1.3. Only the earth plaster E and the cement C_0.9 [28] and C_1.3 [24] also were tested for fresh bulk density [29].

2.2. Hardened State General Test Methods

All the selected mortars and pastes were cast in prismatic moulds measuring 40 mm × 40 mm × 160 mm and cured. As reported by the respective authors: cements and NHL mortars were moulded and cured according to EN 1015-11 [30]; the G and CL_Gs were moulded according to EN 13279-2 [26]; the air lime mortar CL was cured for five days at 20 ± 2 °C and 65 ± 5% RH, and after demoulding was kept in the same conditions. The E specimens were cured for seven days in the moulds at 20 ± 2 °C and 65 ± 5% RH, then demoulded and kept in the same environment for four months (Figure 1a).

**Figure 1.** Clay-based mortar samples: (a) when drying; (b) after flexural test.

After drying, the bulk density was geometrically determined [31]. Flexural strength was evaluated for three prismatic specimens with a 2 kN loading cell and 10 N/s loading speed. Compressive strength of the six semiprisms measuring approximately 40 mm × 40 mm × 80 mm derived from the flexural test (Figure 1b) was determined [30] with a 2 kN loading cell and 50 N/s loading speed. A universal force equipment ETI-HM-S/CPC from PROETI was used for the tests. The dynamic modulus of elasticity was assessed according to EN 14146 [32] using a ZRM ZEUS 2005 to test the frequency of resonance of prismatic specimens. The dry bulk density, flexural, compressive strength, and dynamic modulus of elasticity of all the other

plasters and pastes [21–24] were tested following the same standards used for the earth plaster, with loading cells and speeds suitable for each plaster. Open porosity for cement and lime mortars were measured [22–24] by the hydrostatic method [33], and for CL_G and G [21] by mercury intrusion porosimetry (MIP). Capillarity by water absorption was tested based on EN 1015-18 [34] by Freire [21], Pederneiras et al. [23], and Farinha et al. [24]; and EN 15801 [35] by Santos [22].

2.3. Preparation of the Specimens

For each coating material, the hardened prismatic specimens were mechanically cut, and five specimens measuring approximately 40 mm × 40 mm × 20 mm (Figure 2) were obtained (Table 2).



Figure 2. (a) Prismatic samples of C_1.3; (b) samples that were sliced to obtain specimens measuring 40 × 40 × 20 mm³.

Table 2. Dimensions and mass (average value of 5 specimens) of plaster specimens at the beginning of the experimental campaign.

Pastes and Mortars	Specimens			
	S ₁ (mm)	S ₂ (mm)	d (mm)	Mass (g)
G	40	40	21	34
CL50_G50	40	40	21	34
CL70_G20	38	38	21	29
E	39	40	22	58
CL	40	40	23	57
NHL	40	40	21	55
C_0.9	40	40	22	64
C_1.3	40	40	22	60

Notation: S₁—side 1; S₂—side 2; d—thickness mean value.

Thereafter, the new specimens were prepared to be tested for water vapour permeability [36], adsorption/desorption [25,37], and moisture buffering [8]. The surfaces resulting from the cut were selected to be exposed during the tests.

2.4. Relative-Humidity-Dependent Properties Test Methods

2.4.1. Water Vapour Permeability

Five specimens for each mortar and paste, preconditioned at 20 ± 2 °C and 65 ± 5% RH, were sealed on their edges by aluminium tape and then placed on top of plastic boxes (65 mm × 55 mm × 40 mm) in which a cut of 35 mm × 35 mm was performed. The base (40 mm × 40 mm) of each specimen was then sealed by paraffin wax with the top of the box (Figure 3a). The dry-cup method according to ISO 12572 [36] was followed, and 0% RH inside each box was obtained with 30 mL of calcium chloride (CaCl₂) as desiccant, ensuring the 15 ± 5 mm air space between the desiccant and the lower surface of the specimen. The closure of the box was sealed with paraffin wax (Figure 3b). Before beginning the

experiment, the assembly (box + specimen) was weighed and the starting mass, m_0 , determined. A balance with 0.001 g resolution was used. The specimens were placed in a FITOCLIMA 700EDTU climatic chamber at $50 \pm 5\%$ RH and $23 \pm 5^\circ\text{C}$, and weighed every 24 h until three successive daily determinations of the weight agreed to within 5% and the curve of change in mass against time displayed a constant mass change rate.

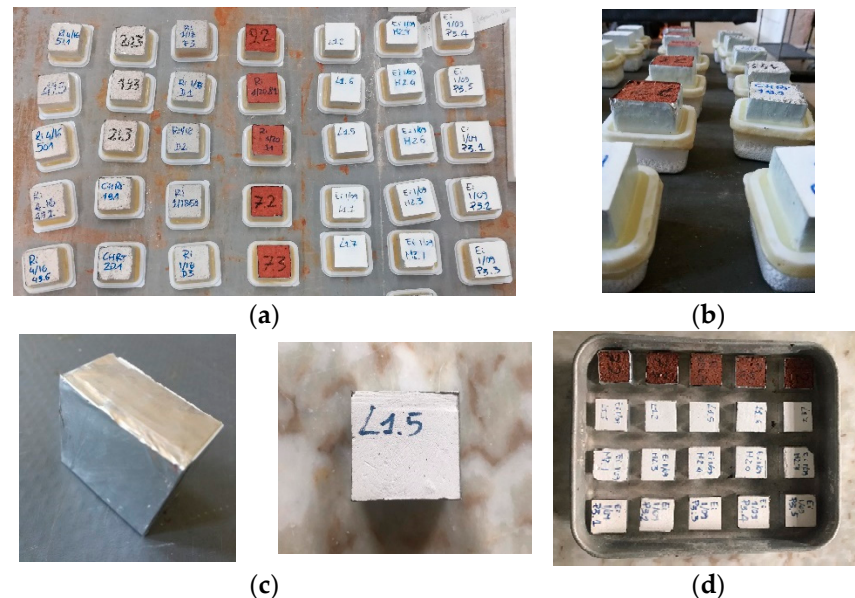


Figure 3. (a) Specimens sealed on the top of the plastic boxes filled with the desiccant; (b) zoom of the specimens sealed for the water vapour test; (c) sealed by aluminum tape; (d) placed in a laboratory tray.

2.4.2. Adsorption/Desorption

The five specimens for each plaster were then sealed on their edges and their bases with aluminum tape (Figure 3c), ensuring only one exchanging surface was exposed. They were used to perform adsorption/desorption according to a simplified version [38] of DIN 18947 [25]. After preconditioning in a climatic chamber (FITOCLIMA 700EDTU) at $50 \pm 5\%$ RH and $23 \pm 5^\circ\text{C}$ until reaching a constant mass, the specimens were weighed and the starting mass, m_0 , was determined. A balance with a 0.001 g resolution was used. The RH was increased to $80 \pm 5\%$, and specimens were weighed after 1, 3, 6, 12, and 24 h. The weighing at 0.5 h prescribed by the standard was not performed to ensure the chamber was stabilized at 80% RH for a substantial period of time before the weighing. The adsorption phase was extended to 24 h, according to the modified version, to better understand the adsorption behaviour of the highly hygroscopic plasters. After 24 h, the climatic chamber was set at $50 \pm 5\%$, $23 \pm 5^\circ\text{C}$, and desorption was run following the same weighting intervals. The results are displayed in g/m^2 against time.

2.4.3. Sorption Isotherms

The hygroscopic curve was determined according to ISO 12571 [37]. The same specimens described in Section 2.4.2 were dried at 60°C until reaching a constant mass and then placed in a climatic chamber. During adsorption, five RH steps (30%, 50%, 70%, 80%, 95%) until reaching equilibrium were performed on the specimens at a constant temperature of $23 \pm 5^\circ\text{C}$. Equilibrium at each stage was reached when the change in mass of three successive weightings, every 24 h, was less than 0.1%. Once adsorption was completed, desorption was performed following the same RH steps from 95% to 30%. Sorption isotherms were obtained from the equilibrium moisture content of each step.

2.4.4. Moisture Buffering Value

Determination of the moisture buffering value (MBV) followed the NORDTEST protocol [8]. The same five specimens for each plaster were dried at 60 °C and the starting mass, m_0 , was determined. The specimens were then placed in a climatic chamber inside a laboratory tray (Figure 3d) to avoid direct air flow. Temperature was fixed at 23 ± 5 °C, and four daily cycles of 33–75% RH were run. The last three cycles were considered to calculate the value. According to the method, loading and unloading phases were respectively kept at 8 h and 16 h, simulating the daily use of one bedroom. MBV was then calculated as the average value of the last three cycles of adsorption and desorption. The results are expressed in $g/(m^2\%RH)$.

3. Results

3.1. Plasters General Characteristics

Table 3 shows the synthesis of the general characteristics of the three pastes and five mortars, and presents the general requirements for compatible plastering substitution mortars for old buildings [18]. The ranges given are meant to be used for a first assessment of compatibility, when no deeper knowledge of the substrate and/or the plaster to replace is available.

Table 3. Synthesis of hardened characterization of plasters.

Pastes and Mortars	Ref.	Test Age	OP (%)	BD (kg/m ³)	Fs (MPa)	Cs (MPa)	DME (GPa)	CC (kg/(m ² min ^{0.5}))	W _{24h} ¹ (kg/m ²)
G	[14]	2 y	46.1	1128	2.42 ± 0.11	5.19 ± 0.27	5.04 ± 0.01	6.42	71.26
CL50_G50	[14]	2 y	48.4	1104	1.61	3.24 ± 0.31	2.35 ± 0.01	6.23	76.26
CL70_G20	[14]	2 y	50.7	1031	1.55	3.03 ± 0.40	1.87 ± 0.00	4.49	78.92
E	–	120 d	–	1743 ± 0.01	0.45 ± 0.04	0.82 ± 0.05	3.50 ± 0.01	–	–
CL	[15]	90 d	25.8	1720	0.39	0.55	2.72	1.71	31.00
NHL *	–	90 d	26.2	1780	0.15 ± 0.02	0.35 ± 0.002	1.86 ± 0.07	2.4	36.50
C_0.9	[16]	28 d	20.2	1919	2.56 ± 0.21	9.66 ± 0.11	16.2 ± 0.9	0.43 *	24.30 *
C_1.3	[17]	2 y	22.4	1875	2.00 ± 0.31	5.98 ± 0.79	10.1 ± 0.8	1.55 (1 y)	17.47 ² (1 y)
Requirements	[18]	–	–	–	0.20–0.70	0.40–2.50	2.00–5.00	–	–

Notation: OP—open porosity; BD—bulk density; Fs—flexural strength; Cs—compressive strength; DME—dynamic modulus of elasticity; CC—capillary water absorption; W_{24h}—water absorption at 24 h; d—days; y—years; ±—values for standard deviation; *—unpublished result; ¹—dimensions of 40 × 40 × 160 (mm); ²—dimensions of 40 × 40 × 80 (mm).

The open porosity (OP) and dry bulk density (BD) of the pastes and the mortars differed greatly. According to the WTA directive 2-9-04/D (cited by Pavlíková et al. [39]) for restoration renders, the dry bulk density should be guaranteed below 1400 kg/m³, and the open porosity above 40%. Thus, if applying these limits to the analysed plasters, only the three pastes fulfilled the requirements. Moreover, the cement-based mortars presented the highest values of compressive strength, as expected, followed by the gypsum-based pastes, the clay, the air lime, and the natural hydraulic lime mortars. All the plastering mortars fulfilled the general requirements for compressive strength [1] within different classes except the NHL plaster, which was slightly below the lowest class CSI (0.4 to 2.5 N/mm²). If considered for use as restoration products instead, only E and CL fit the compatibility range, with NHL placed slightly below and all the other pastes and mortars above the range. As for the compressive strength, the highest value of dynamic modulus of elasticity was observed for the C plasters, and the lowest for the NHL one. Only the CL_G pastes presented a lower value than expected from the observation of their mechanical properties. The values could depend on their different pore microstructures. The pastes' capillary water absorption coefficient was very high, as was the free water saturation. The predominance of the capillary pores in their pore structure, characteristic of the permeable binders used and linked to the absence of sand, may explain the high capillary rise. Between the mortars, the highest capillary water absorption coefficient was observed for the NHL and the lowest for the cement mortar. Considering the range of values suggested for compatibility, the mechanical behaviour of the E, CL, and NHL plasters fulfilled the requirements, unlike

both cement plasters, as expected. Hence, if applying these cement mortars as substitutive interior plasters, they could transmit a higher stress to the pre-existing material and accelerate the degradation phenomena. The physical compatibility concerns the behaviour of the liquid and vapour phases of water; retention of water in the substrate or in the pre-existing mortars could trigger new degradation mechanisms, especially if soluble salts are introduced with the repair mortar. Capillary water absorption and water vapour permeability should be high enough to guarantee water migration and evaporation. Thus, considering the inferior limit of $1.0 \text{ kg}/(\text{m}^2 \text{ min}^{0.5})$ of capillary water absorption suggested for renders [18], the C_0.9 specimen did not fulfil the requirement for physical compatibility, and would be the less-feasible choice for substitution in old buildings.

3.2. Water Vapour Permeability

Table 4 shows the main values for the water vapour permeability (WVP) of the analysed coating materials and for the resistance factor, calculated as the ratio between the WVPs of air and plaster (δ_a/δ_p). The WVP of air (δ_a) refers to the Shirmer formula, equal to 1.951×10^{-10} . The combinations of air lime and gypsum, namely CL70_G20 and CL50_G50, showed the highest value of WVP (δ_p), followed by gypsum and air-lime-based ones. The high WVP of gypsum and gypsum–lime agreed with the study of Ramos et al. [9], in which the same test procedure was applied to larger specimens (210 mm \times 210 mm, with a thickness of 20 mm and 10 mm, respectively). A lower WVP was observed in mortars based on NHL and earth. The lowest values were presented by the cement mortars. The C_1.3 specimen, with a higher w/b ratio and longer curing, showed higher permeability than the C_0.9 specimen, which can be explained by the more porous microstructure of the latter. Furthermore, considering the limit of the 0.10 m thickness of the equivalent air layer (Sd, d = 10 mm) recommended for substitution plasters in old buildings [18], none of the cement-based plasters was suitable for this type of application. In addition, the EN 998-1 specification [1] and the WTA directive 2-9-04/D (cited by Pavlíková et al. [39]) define a limit for WVP, requiring a water vapour resistance factor (μ) ≤ 15 and <12 , respectively, for renovation mortars. Hence, the requirement was not fulfilled by both cement mortars when considering the directive, and only by C_0.9 according to the standard.

Table 4. Synthesis of results of WVP (including standard deviation) for all the plasters.

Pastes and Mortars	d (mm)	ΔM 24 h (g)	Q ((kg/s) $\times 10^{-9}$)	Wp (ng/m ² ·s·Pa)	WVP (kg/(m·s·Pa))·10 ⁻¹²	μ (-)	Sd (m)
G	20.69	0.30	3.43	1718	35.53 ± 1.2	5.49	0.055
CL50_G50	21.06	0.30	3.54	1775	37.36 ± 1.2	5.22	0.052
CL70_G20	20.91	0.29	3.38	1802	37.68 ± 1.6	5.18	0.051
E	22.43	0.15	1.69	960	21.50 ± 0.8	9.07	0.091
CL	22.52	0.20	2.31	1166	26.24 ± 0.5	7.43	0.074
NHL	21.12	0.17	1.97	991	20.92 ± 0.8	9.32	0.093
C_0.9	22.01	0.07	0.86	434	9.55 ± 0.8	20.42	0.204
C_1.3	21.59	0.11	1.25	624	13.48 ± 1.2	14.48	0.144

Notation: d—thickness; ΔM —daily change in mass; Q—water vapour flow; Wp—water vapour permeance; WVP—water vapour permeability; μ —water vapour resistance factor; Sd—thickness of the equivalent air layer (for d = 10 mm).

The dimensional variation of specimens from the requirements of the WVP standards [36] mostly concerned the exposed area. Indeed, the prescription was to use a specimen with a diameter or side at least two times its thickness, and with a minimum exposed area of 5000 mm². The 20 mm thick and nearly 40 mm side specimens produced for the study complied with the first prescription. The exposed area; i.e., “the arithmetic mean of the upper and lower free surface areas” [36], instead, was roughly 3000 mm². However, the dimension of specimens hugely differed from study to study, in each of which the same testing method was applied, and the exposed surface varied from a minimum of about 17,318 mm² [40] to a maximum of nearly 88,200 mm² [9]. The possibility

of introducing uncertainties in measurements was higher for smaller specimens, thus the number of specimens was increased from three to five, and a comparison with previous studies was run to confirm the accuracy of the results. Hence, Table 5 reports values of WVP and resistance factor determined by dry cup from the literature [40–50]. For clay- and air-lime-based plasters, the consistent difference between the dry and wet methods has previously been shown by some authors [43,45–47], with values of resistance factor determined by dry cup two times higher than by wet cup, but no evidence of this difference was found for cement mortars. Therefore, due to the lack of results from dry-cup testing found in literature, the cement mortar range refers to the wet-cup test method. In the comparison, the WVP of the tested plasters was higher than the referred range (or value where only one study was found) and, consequently, the resistance factor was lower, except for cement. However, the composition of the mortars and pastes from the literature showed a consistent heterogeneity even if based on the same binders, due to the additions of diverse materials and/or natural fibers, or even due to different w/b ratios.

Table 5. Comparison with the literature of the water vapour permeabilities and resistance factors obtained by the dry-cup test method.

Pastes and Mortars	WVP (10^{-12} kg/(m·Pa·s))			Resistance Factor μ (–)		
	Result		Range *	Result		Range *
Gypsum	35.5	▲	21.9–29.2	5.5	▼	7.0–9.1
Gypsum + lime	37.4	▲	28.9	5.2	▼	6.7
	37.7	▲		5.2	▼	
Clay	21.5	▲	7.8–8.8	9.1	▼	22.1–25.0
CL90	26.2	▲	5.3–16.0	7.4	▼	12.2–37.1
NHL3.5	20.9	▲	9.9	9.3	▼	19.6
Cement **	9.5		4.9–14.0	14.5		13.9–40.0
	13.5			20.4		

Notation: *—values from the literature [33–44], due to the lack of results for permeability or resistance factor in some cases, were calculated using δa of 19.50×10^{-11} (kg/(m·Pa·s)); ▲—value above the range; ▼—value below the range; **—range from the literature for cement refers to the wet-cup test method.

The pastes *G*, *CL50_G50*, and *CL70_G20* are compared in Table 6, with values reported by Freire [21] after testing WVP according to EN 1015-19 [51] by wet cup, at 90 days and 2 years of curing of the same. It is expected that the wet-cup method will return higher values of WVP than the dry-cup method; however, pastes with the presence of lime showed a higher permeability in the later test, probably related to an increase in porosity over time. Nevertheless, the equivalent air layer for 10 mm of thickness (*Sd*) complied with the limit of 0.10 m [18] either by wet or dry cup.

Table 6. Comparison with results from the study of Freire [21] of water vapour permeability and equivalent air layer for a thickness of 10 mm tested by wet cup [51].

Pastes	Test Age	WVP (kg/(m·Pa·s)) E-11		Sd (m) (d = 10 mm)	
		Wet Cup	Dry Cup (8 y)	Wet Cup	Dry Cup (8 y)
G	90 days	4.915	3.553	0.035	0.055
	2 years	3.169		0.057	
CL50_G50	90 days	2.036	3.736	0.100	0.052
	2 years	2.397		0.083	
CL70_G20	90 days	3.282	3.768	0.054	0.051
	2 years	2.269		0.081	

Notation: WVP—water vapour permeability; Sd—equivalent air layer; d—specimen thickness.

3.3. Adsorption/Desorption

Figure 4 displays the mean curve of adsorption and desorption for each plaster, and the limits of the three classes defined by DIN 18947 [25]. The clay plaster *E* showed high hygroscopic behaviour, adsorbing 74.4 g/m^2 at 12 h, about 15 g/m^2 higher than the highest class of the standard WSIII ($\geq 60 \text{ g/m}^2$). The maximum adsorption, at 24 h, was 99.3 g/m^2 ,

in accordance with another study that tested the same premixed clay plaster [52]. The residual moisture content at the end of the test was 16.1 g/m^2 . The test was therefore extended, and after additional 48 h (96 h from the beginning of sorption phase), the residual moisture content was 4.7 g/m^2 . The temporal relation between adsorption and desorption could be 1 to 3 or more. The pastes based on air lime and gypsum (*CL70_G20*, *CL50_G50*) showed higher hygroscopicity than pure G paste and CL mortar, but a similar curve after the first 6 h. The low hygroscopic behaviour of the air lime mortar (*CL*) was evident, mainly when compared with the *CL70_G20* paste. This could be due to the absence of sand and the different microstructure. The slope of their curve at the end of adsorption was lower than for the cement-based mortars, and they probably could have adsorbed more if they were loaded longer. After 48 h, at the end of the desorption process, all the tested coatings showed a residual value of uptaken moisture. The *C_0.9* and *C_1.3* specimens showed the slowest desorption, confirming a low hygroscopic performance of the cement plasters.

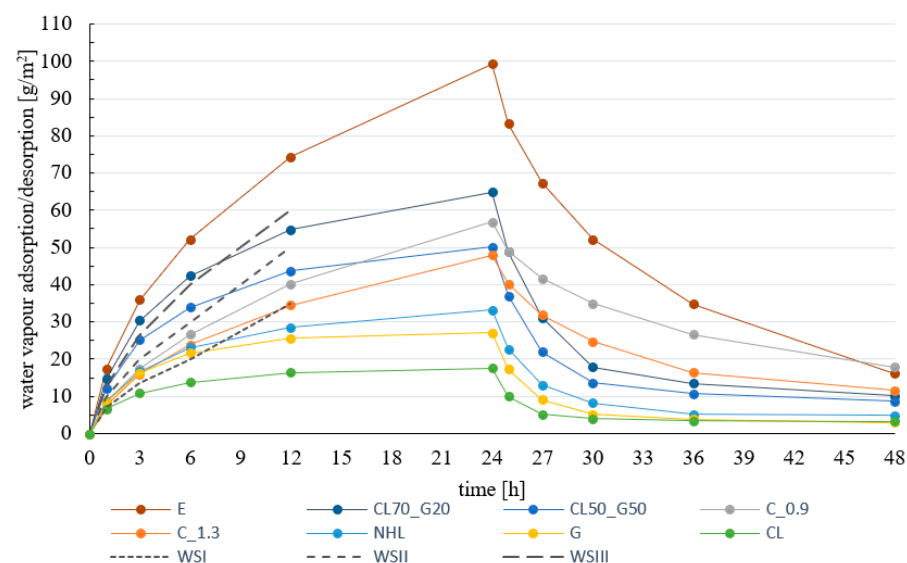


Figure 4. Sorption and desorption curve of plasters and hygroscopic classes of WS defined by DIN 18947 [25].

In the test, a nonsignificant coefficient of variation (CV) was observed between specimens, except for G and CL. The air lime specimens presented a maximum CV of 14% at the end of 24 h of adsorption, and the gypsum specimens presented 61%. Thus, the gypsum paste displayed a significative dispersion between the five specimens. The test was run two times, and similar results were obtained. Based only on the similar response of three specimens, the average value of adsorption was 17.6 g/m^2 at 24 h, and final moisture content at 24 h of desorption was 2.1 g/m^2 , which agreed with studies of other authors [52]. The possible explanation is that the highest hygroscopic performance corresponded to specimens obtained from the topmost regions of the original sample, while the lowest corresponded to specimens obtained from the core of the prism. In this context, the highest value would better represent a real application. Regardless, an operational error was excluded with the support of the repetition of the test, thus the average curve in Figure 4 includes all the samples.

Table 7 compares results among several authors who tested adsorption and desorption according to DIN 18947 [25] or the modified version of it (adsorption extended to 24 h and an inverse process for desorption). As the standard addresses earth plasters, only one study was found [52] testing premixed gypsum and cement mortars. All the other values were from earth-based plasters differing in clay mineralogy, sand granulometry, and fibers. Most of the studies used specimens with a similar thickness (15–20 mm), but a very different exposed area ($500 \text{ mm} \times 200 \text{ mm}$) when compared to the present study. Although there was a difference in specimen dimensions, the results obtained from our

study were in agreement with the ones found in literature, implying that using smaller specimens may be a viable option.

Table 7. Synthesis of adsorption and desorption results (with standard deviation) and comparison with other studies from the literature.

Plaster		Adsorption (g/m ²)		Desorption (g/m ²)		Ref.
		(12 h)	(24 h)	(12 h)	(24 h)	
Clay	Ep	74.43 ± 4.42	99.35 ± 4.89	34.76 ± 1.56	16.10 ± 1.51	Present study
		<80	104	>10 and <20	<10	[52]
		>60	–	≈0	–	[53]
		<130	–	≈60	–	[53]
		67.7	–	–	–	[54]
		68.5	–	–	–	[54]
		105.3	–	–	–	[54]
		>60 and <80	–	–	–	[55]
		>80 and <100	–	<20	–	[53]
	Ef	<70	≈ 80	≈12	≈ 5	[56]
		>21 and <38	-	0	-	[57]
		>60	76	<10	<5	[52]
		≈80	–	≈ 0	–	[53]
		≈100	–	≈20	–	[53]
		≈60	>70	>10	<15	[58]
		≈70	≈85	≈18	>10	[58]
		≈80	<100	<25	>10	[58]
	E	≈85	≈110	≈30	–	[58]
		<70	≈ 85	≈ 20	≈10	[56]
		≈80	≈83	≈ 10	≈0	[59]
		≈60	≈78	–	–	[59]
Cement		60	70	>10 and <20	<10	[38]
		30	–	0	–	[57]
	E _K	30	35	≈0	0	[38]
	E _B	110	140	>30 and <40	≈10	[38]
	C	34.49 ± 3.02	47.99 ± 7.79	16.45 ± 2.13	11.54 ± 2.14	Present study
Gypsum		40.21 ± 3.45	56.84 ± 5.27	26.59 ± 3.15	17.89 ± 2.06	Present study
		40	40	≈0	≈0	[52]
	G	25.54 ± 13.42	27.15 ± 16.62	3.90 ± 2.54	3.03 ± 1.96	Present study
	G	22	22	≈0	≈0	[52]

Notation: E—illitic clay mortar; Ef—illitic clay mortar with natural fibers; Ep—premixed illitic clay mortar; E_K—kaolinitic clay mortar; E_B—montmorillonitic clay mortar; C—cement mortar; G—gypsum mortar. Values reported using symbols ">", "<", or "≈" were taken from graphs; ±—values for standard deviation.

3.4. Sorption Isotherms

The average change in mass (u) of each plaster for every RH step is presented in Figure 5. The dry state was chosen as starting point for adsorption, but in the desorption phase, a 0% RH was not possible to obtain, thus the curves are not closed. The results for CL70_G20 and CL50_G50 are shown separately (Figure 5b), due to the consistently higher values of water vapour adsorbed during the last RH stage (95%) and residual moisture content at 30% RH. The clay-based plaster (Figure 5a) showed the highest hygroscopicity at each step, if compared with mortars based on cement, gypsum, air lime, and natural hydraulic lime. Above 80% RH, the slope of the equilibrium moisture content curve of cement mortars C_0.9 and C_1.3 and air lime–gypsum pastes CL70_G20 and CL50_G50 slightly rose. The presence of air lime in the CL_G pastes, if compared with pure gypsum paste, showed a significant increase of adsorption above 80% RH and hysteresis in desorption. The CL_G specimens were analysed by MIP after 90 days and 2 years of curing [21], and a direct connection was found between the lime content and the amount of smaller pores in the range of 0.1–0.5 micron. Given that this range was found more sensitive to condensation of water adsorbed (Houst and Wittmann, 1994 cited by Freire [21]), the high adsorption at 95% RH probably was due to capillary condensation, as also observed by

other authors [9]. The presence of liquid water in pores could have possibly given access for CO_2 in a dissolved state to react with $\text{Ca}(\text{OH})_2$, initiating the precipitation of CaCO_3 . Furthermore, the slices cut from prismatic specimens could have exposed the inner core that was still not completely carbonated. Although samples with CL were aged previous to testing, a pH test could not be performed for confirmation. The long amount of time taken to reach equilibrium at a high RH level and the change in mass kept from these two plasters after the test suggested that a faster carbonation of calcium hydroxide occurred, probably promoted by a high RH [60].

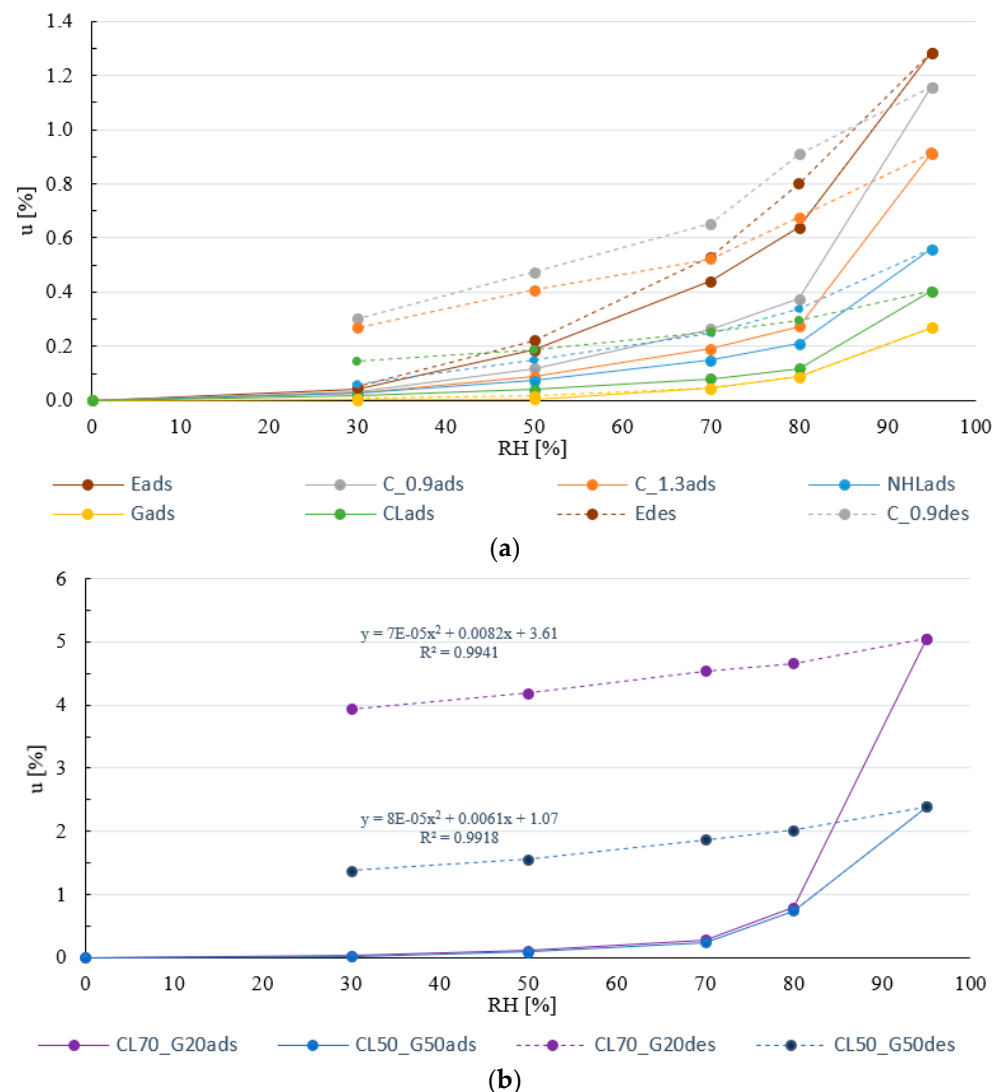


Figure 5. Average change in mass for each mortar and paste per RH step, tested according to ISO 12571 [30].

Values of the standard deviation were not high, except for CL and G, as expected according to the previous test of adsorption/desorption. The air lime mortar (CL) presented a high variation in adsorption only after 80% RH exposure and during the entire desorption phase. The response of the G specimens was similar to that observed in the previous section, confirming the hypothesis of the heterogeneity of the original prismatic sample, and as such, for the same reasons presented above, all specimens were considered reliable.

Results for the hygroscopic behaviour of G, CL70_G20 and CL50_G50 were compared with the ones obtained by Freire [21] using the same methodology on the same pastes after 2 years of curing (instead of 8 years), although in that study the RH passed from 70% to 90%, while in the present study it rose to 80% and afterward to 95% RH. Furthermore, the

specimens tested at 2 years were unsealed circular truncated cones with a bottom diameter of 50–55 mm, top diameter of 55–60 mm, and thickness of 15–18 mm. The results (Table 8) are given in % by mass. Major differences were observed for the highest step of RH reached. The difference of 5% between the highest RH stages tested in the two studies seemed to widely affect the equilibrium moisture content of all the pastes, which at 95% RH, rose to approximately 2.5 times the value registered at 90% RH (in bold in Table 8), together with a sudden increase in the standard deviation. This effect is evident in Figure 6: the curves of the two studies are almost overlaid for RH levels below 80%. Instead, above 80% RH, the higher the content of air lime, the higher the increase of the moisture adsorbed, and thereby of the residual moisture content. The pure gypsum paste did not show the same adsorption capacity than the air lime–gypsum pastes. In both studies (2 years and 8 years), the hygroscopicity of G was quite low, and a slight rise of the curve was observed in the oldest paste.

Table 8. Synthesis of adsorption and desorption results (8 years) and comparison with the study of Freire [21] (2 years).

MC (%)	CL70_G20				CL50_G50				G			
	8 y		2 y		8 y		2 y		8 y		2 y	
	AV	SD	AV	SD	AV	SD	AV	SD	AV	SD	AV	SD
30	0.03	0.003	0.05	0.004	0.02	0.002	0.06	0.004	0.02	0.002	0.03	0.003
50	0.11	0.004	0.09	0.049	0.10	0.002	0.11	0.005	0.06	0.005	0.06	0.003
70	0.28	0.004	0.16	0.059	0.24	0.006	0.19	0.003	0.14	0.046	0.08	0.003
80	0.80	0.074	—	—	0.74	0.036	—	—	0.21	0.090	—	—
90	—	—	1.67	0.037	—	—	1.30	0.094	—	—	0.18	0.009
95	5.05	0.129	—	—	2.39	0.172	—	—	0.48	0.270	—	—
80	4.66	0.180	—	—	2.03	0.185	—	—	0.25	0.088	—	—
70	4.54	0.237	1.44	0.036	1.87	0.185	1.09	0.096	0.17	0.044	0.10	0.008
50	4.19	0.260	1.33	0.037	1.56	0.176	1.00	0.094	0.08	0.017	0.07	0.007
30	3.94	0.267	1.17	0.035	1.37	0.179	0.84	0.092	0.03	0.006	0.04	0.008

Notation: MC—moisture content; y—years of curing; AV—average value; SD—standard deviation.

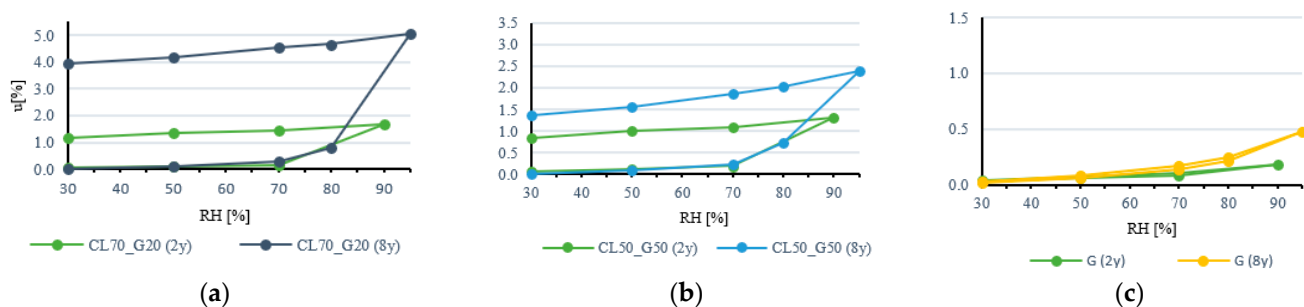


Figure 6. Synthesis of adsorption and desorption results (8 years) and comparison with the study of Freire [21] (2 years) for: (a) CL70_G20; (b) CL50_G50; and (c) G pastes.

3.5. Moisture Buffering Value

The mean values of MBV for adsorption and desorption calculated for the last three cycles for all the tested plasters are presented in Figure 7.

Classes of MBV proposed by Rode et al. [8] were useful for a quick comparison of different materials. Above 2 g/(m²%RH), the behaviour was classified as excellent, but here is not referred, as none of the considered materials exceeded the *good* grade. The highest values of moisture buffering observed were from clay plaster and air lime–gypsum pastes, which showed a *good* behaviour (1 < MBV < 2 g/(m²%RH)) according to the limits suggested by Rode et al. [8]. NHL and cement plasters showed a similar MBV, classified as *moderate* (0.5 < MBV < 1 g/(m²%RH)). The lowest values were observed for G, but it was still classified as *moderate*, although showing a very high standard deviation; and CL was ranked as *limited* (0.2 < MBV < 0.5 g/(m²%RH)).

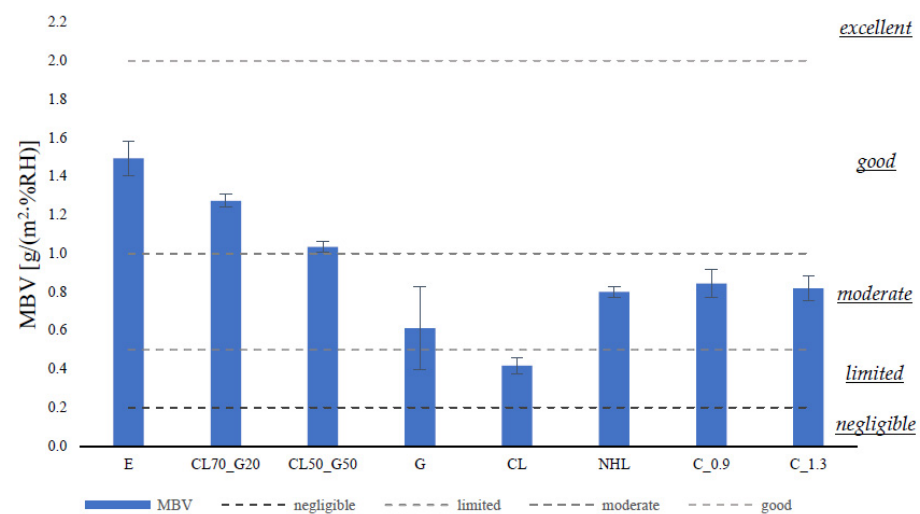


Figure 7. MBV of tested plasters (and standard deviation) and limits from NORDTEST [8].

Several other studies used the NORDTEST method to test plasters' MBV. A finishing coating paste based on gypsum and another composed of 50% gypsum and 50% air lime (by weight) were tested by Ramos et al. [9] with specimens measuring 210 mm × 210 mm × 20 mm and 210 mm × 210 mm × 10 mm, respectively. Values of MBV at 23 °C were 0.47 g/(m²·%RH) for gypsum–lime pastes and 0.72 g/(m²·%RH) for pure gypsum pastes. The MBV found for CL50_G50, 1.03 g/(m²·%RH), was consistently higher than the one found by Ramos et al. [9], while for G (0.61 g/(m²·%RH)), the values were closer. Cascione et al. [42] tested clay, light-weight gypsum, and NHL3.5 plasters. The tested clay was kaolinitic; the mortar had a 20% mass of water, the binder:aggregate ratio of the NHL plaster was 1.2:5, and the hemi-hydrate gypsum mortar had a 30% mass of water. The dimensions of the specimens were 150 mm × 150 mm × 20 mm. The results obtained were 1.67, 1.60, and 0.95 g/(m²·%RH), respectively, for the clay, gypsum, and NHL plasters. The values for clay and NHL were slightly higher than those obtained in the present study (1.49 and 0.80 g/(m²·%RH), respectively), but the gypsum was almost three times higher. An unknown complete composition of the light-weight gypsum tested by Cascione [42] may explain the different response of two gypsum-based coatings. According to Roels et al. [61], for a gypsum plaster, the thickness involved in the mechanism of moisture buffering is approximately 33 mm, and when thinner samples are tested, the MBV drops. Thus, considering that the results from Cascione et al. [42] and the present study were both from specimens of about 20 mm thickness, it was expected that their thicknesses were completely involved in moisture buffering, and samples showed a different percentage of the potential response of each plaster. Nevertheless, there was no experimental proof in this study that a thicker G sample would respond with a higher MBV. Regardless, the different composition and microstructure was considered here as mainly responsible for the different behaviours. A cement CEM II A/LL 42.5 R plaster was tested by Giosuè et al. [49] with a volumetric binder: aggregate proportion of 1:3.5, using cylindrical specimens with a diameter of 100 mm and a thickness of 30 mm. The MBV found was about 0.3 g/(m²·%RH), much lower than the values of 0.82 and 0.84 g/(m²·%RH) found in the present study, and enough to obtain different ratings in the MBV classification. The cement plasters had similar composition, except the one tested by Giosuè et al. [49], which showed a slightly higher dry bulk density (2091 kg/m³) and a lower flow table consistency (120 mm). Thus, the thickness, porosity, and dry bulk density seemed to be parameters of influence for this test, rather than the dimensions of specimens, contributing to confirming the reliability of the tests using small samples.

4. Discussion

A synthesis of the characterization of RH-dependent properties for the eight analysed plasters is presented in Table 9. The same test procedures were adopted for all the plastering mortars and pastes, guaranteeing comparability of results.

Table 9. S Synthesis of average results of WVP, adsorption/desorption, sorption isotherms, and MBV.

Pastes and Mortars	WVP (kg/(m·s·Pa)) × 10 ^{−12}	MC _(12 h) (g/m ²)	MC ₃₀ (%)	MC ₅₀ (%)	MC ₇₀ (%)	MC ₈₀ (%)	MC ₉₅ (%)	MC ₈₀ (%)	MC ₇₀ (%)	MC ₅₀ (%)	MC ₃₀ (%)	MBV (g/(m ² %RH))
G	35.53	25.5	0.02	0.06	0.14	0.21	0.48	0.25	0.17	0.08	0.03	0.61
CL50_G50	37.36	43.6	0.02	0.10	0.24	0.74	2.39	2.03	1.87	1.56	1.37	1.03
CL70_G20	37.68	54.8	0.03	0.11	0.28	0.80	5.05	4.66	4.54	4.19	3.94	1.27
E	21.50	74.4	0.04	0.19	0.44	0.64	1.29	0.80	0.53	0.22	0.05	1.49
CL	26.24	16.5	0.02	0.04	0.08	0.12	0.40	0.30	0.25	0.19	0.14	0.42
NHL	20.92	28.6	0.03	0.07	0.15	0.21	0.56	0.34	0.25	0.15	0.06	0.80
C_0.9	9.55	40.2	0.03	0.12	0.26	0.38	1.16	0.91	0.65	0.47	0.30	0.84
C_1.3	13.48	34.5	0.03	0.09	0.19	0.27	0.91	0.68	0.52	0.41	0.27	0.82

Notation: WVP—water vapour permeability; Δm —change in mass; A—exchanging surface; MC—moisture content; MBV—moisture buffering value; E—clay; G—gypsum; CL—air lime; NHL—natural hydraulic lime 3.5; C—cement.

All the pastes showed a WVP higher than the mortars, and the CL_G pastes presented a higher WVP than pure G and CL mortars. When the RH passed from 50% to 80% and was kept for 12 h [25], the highest adsorption was performed by the clay mortar (74.4 g/m²), followed by the CL_G pastes and C mortars. When tested in a steady state from 50% RH to 80% RH (Table 9), the moisture content of the E mortar rose less than that of the CL_G pastes. Thus, also considering the MBV found, the plaster based on clay had a quicker response to adsorption. The clay plaster E showed results in agreement with the literature for WVP and hygroscopic behaviour. The measured MBV confirmed the good response to moisture buffering of clay. Cement mortars showed the lowest WVP between the analysed plasters, in agreement with previous studies [50] performed using the wet-cup method, whereas adsorbed water vapour at 12 h of 80% RH exposure was the highest for the E and CL_G plasters, and a high moisture content was displayed in the sorption isotherms at 95% RH (still lower than E and CL_G). As discussed in the previous section, the desorption of cement plasters was a slower process, and they showed hysteresis at the end of desorption. In a steady state, the residual moisture content of C was, after E and the CL_Gs, the highest. Values of moisture buffering found were in accordance with all other tests of hygroscopicity. The two cement and the NHL plasters displayed a similar value of adsorption after 8 h at high RH. Therefore, the similar MBV of these three plasters was related to the specific exposure time and RH prescribed by NORDTEST. NHL and CL presented similar sorption isotherms, and only air lime showed high residual moisture content.

Between the two cement mortars, C_1.3, with higher open porosity (+2.2%), displayed the highest WVP, but a lower hygroscopic behaviour and moisture buffering. The results were in agreement with expectations, considering the need for water was more related to macroporosity than to the sorption mechanism, which involves micro- and mesopores [62]. An analysis of pore size distribution was not run in the present study, but Figure 8 shows this property for the same binder-based plasters (not applied on any substrate, such as in the present study), together with the IUPAC classification of pores and ranges of pores responsible for different mechanism, as presented by Thomson [62].

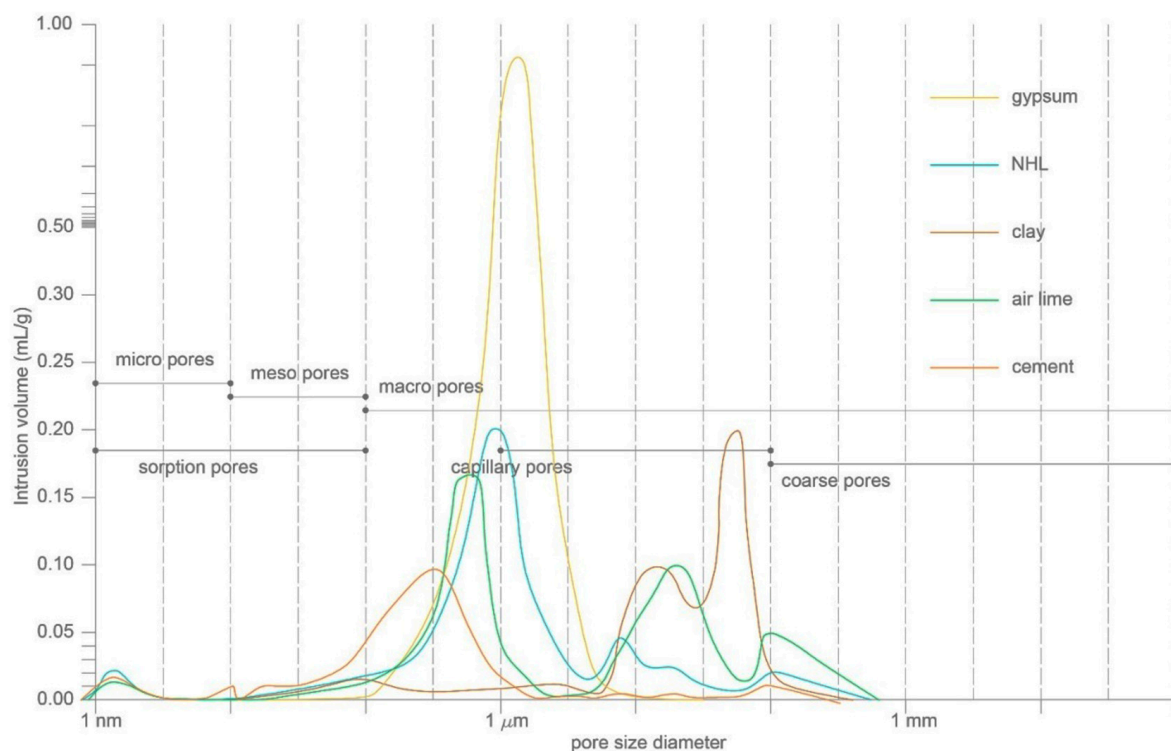


Figure 8. Pore size distribution from the literature [22,63,64] for mortars based on gypsum, natural hydraulic lime, clay, air lime, and cement; and classification and ranges of pores (adapted from IUPAC (1972) and Thomson et al. [62]).

Although the pore size distribution displayed was not obtained from the analysed mortars, it was expected that the contribution of moisture buffering of the *Cs*, *NHL*, and *CL* mortars was quite poor due to the similar and small amount of micropores found for the same type of binder-based mortars [22]. However, the cement mortars showed the highest moisture capacity between them, probably related to their higher amount of mesopores (as shown in Figure 8). Thus, in this case, mesopores of the cement mortars could be responsible for their higher moisture adsorption. Clay plasters [57] showed a higher pore size diameter (in the range of 10^1 – 10^2 μm) in a bimodal distribution, although their pore dimensions did not influence the sorption in the same way, since a chemical mechanism [58] is also responsible for moisture capacity.

5. Conclusions

In the present study, an assessment of RH-dependent properties of five plastering mortars and three finishing pastes was conducted. The general characterizations of the mortars and pastes were discussed and, where applicable, the requirements for substitution plasters for historic buildings were presented, and the prescribed limits and ranges considered. The study was run on two finishing pastes based on air lime and gypsum in different proportions (*CL70_G20* and *CL50_G50*), one gypsum paste (*G*), one plastering mortar based on clayish earth (*E*), one with air lime (*CL*), one with natural hydraulic lime 3.5 (*NHL*) and two with cement (*C_0.9* and *C_1.3*). Apart from *E*, produced for the study, the samples of all the other mortars were received as leftovers from previous experimental campaigns, and thus had different curing ages, all higher than 2 years.

The results led to the following conclusions:

- The three finishing pastes, designed for restoration of historic plaster finishings, showed an open porosity and dry bulk density compatible with requirements for restoration plasters, a mechanical strength above the limit, and a good water vapour permeability for that type of application. The high compressive and flexural strength decreased with the addition of air lime, together with an increase in hygroscopicity. Hence, for moisture passive regulation, the combinations of gypsum and air lime were more suitable than the pure gypsum paste. The latter indeed presented a very low moisture capacity: in static condition, the maximum value of moisture adsorbed was the lowest between all the tested coatings; after 12 h of adsorption, it was probably saturated, and no additional moisture was adsorbed, which was reflected in a *moderate* moisture buffering value. The CL_Gs, instead, presented a *good* moisture buffering, and also were very suitable for passive regulation.
- The earth plaster *E* fulfilled the requirements for mechanical compatibility, together with some of the requirements for physical compatibility with water vapour. There was no doubt that this plaster was the most suitable for moisture passive regulation: it showed high hygroscopicity in dynamic and static conditions. Adsorption capacity exceeded the 24 h test, and it was classified as *good* for moisture buffering.
- The NHL plaster, in terms of compatibility, complied with the same requirements as the earth plaster. Concerning the RH-dependent properties, when tested for adsorption/desorption in static and dynamic conditions, its behaviour was moderately good. Moreover, it showed a moisture buffering value similar to the cement plasters.
- The CL plaster met the mechanical requirement for compatibility, and its water vapour permeability was considered adequate for application as a restoration plaster. Its adsorption and desorption were the lowest when tested dynamically, and were still very low when tested in steady states. Furthermore, its moisture buffering value was the lowest, classified as *limited*.
- The cement plasters were the least suitable for application in historical buildings, as expected. They did not comply with any of the requirements, especially the C_0.9, which was considered the least-compatible choice for substitution in old buildings. They showed the lowest water vapour permeability and slow adsorption and desorption, but their moisture content at high RH was quite significant when tested in a steady state. Their *moderate* classification for moisture buffering made these plasters a possible choice for application in modern building where their passive regulation can be improved.

Further studies, specifically on microstructure, may deepen the understanding of the weak contribution of air lime and pure gypsum plastering mortars and finishing pastes.

Author Contributions: Conceptualization, investigation, writing—original draft preparation, A.R.; supervision, writing—review and editing, P.F.; supervision, writing—review and editing, M.d.R.V. All authors have read and agreed to the published version of the manuscript.

Funding: This research was funded by the Portuguese Foundation for Science and Technology: 1st author Doctoral Training Programme EcoCoRe, grant number PD/BD/150399/2019; and Civil Engineering Research and Innovation for Sustainability Unit-CERIS (UIDB/04378/2020).

Acknowledgments: The authors would like to thank the National Laboratory for Civil Engineering of Portugal (LNEC) for the laboratory equipment and the support provided through the projects PRESERVE and REUSE; the technical team of NRI, especially Bento Sabala; and the researchers who donated their samples, namely Ana Rita Lopes dos Santos, Catarina Brazão Farinha, Cinthia Maia Pederneiras and Maria Teresa Freire.

Conflicts of Interest: The authors declare no conflict of interest.

References

1. *Specification for Mortar for Masonry—Part 1: Rendering and Plastering Mortar*; EN 998-1; European Committee for Standardization: Brussels, Belgium, 2003.
2. Veiga, R. Air lime mortars: What else do we need to know to apply them in conservation and rehabilitation interventions? A review. *Constr. Build. Mater.* **2017**, *157*, 132–140. [CrossRef]
3. Freire, M.T.; Veiga, M.D.R.; Silva, A.S.; de Brito, J. Studies in ancient gypsum based plasters towards their repair: Physical and mechanical properties. *Constr. Build. Mater.* **2019**, *202*, 319–331. [CrossRef]
4. Candeias, A.E.; Nogueira, P.; Mirão, J.; Santos, A.S.; Veiga, R.; Gil, M.C.; Ribeiro, I.; Seruya, A.I. Characterization of ancient mortars: Present methodology and future perspectives. In Proceedings of the Workshop on Chemistry in the Conservation of Cultural Heritage: Present and Future Perspectives, Perugia, Italy, 19–22 March 2006; p. 4.
5. Gomes, I.; Faria, P. Repair mortars for rammed earth constructions. In Proceedings of the XII DBMC 12th International Conference on Durability of Building Materials and Components, Porto, Portugal, 12–15 April 2011; p. 2208, ISBN 9789727521326.
6. Veiga, R.; Faria, P. The role of mortars in the durability of ancient walls. In Proceedings of the CirEA2018 Conferência Internacional Sobre Reabilitação de Estruturas Antigas de Alvenaria, Lisboa, Portugal, 5 June 2018; pp. 1–15, ISBN 978-972-8893-67-5. (In Portuguese)
7. Padfield, T. Humidity buffering of the indoor climate by absorbent walls. In Proceedings of the 5th Symposium on Building Physics in the Nordic Countries, Göteborg, Sweden, 24–26 August 1999; Volume 2, pp. 637–644.
8. Rode, C.; Peuhkuri, R.H.; Mortensen, L.H.; Hansen, K.K.; Time, B.; Gustavsen, A.; Ojanen, T.; Ahonen, J.; Svennberg, K.; Harderup, L.E.; et al. *Moisture Buffering of Building Materials*; BYG Report R-127; Technical University of Denmark, Department of Civil Engineering: Lynby, Denmark, 2005.
9. Ramos, N.; Delgado, J.; de Freitas, V. Influence of finishing coatings on hygroscopic moisture buffering in building elements. *Constr. Build. Mater.* **2010**, *24*, 2590–2597. [CrossRef]
10. Arundel, A.V.; Sterling, E.M.; Biggin, J.H.; Sterling, T.D. Indirect health effects of relative humidity in indoor environments. *Environ. Health Perspect.* **1986**, *65*, 351–361. [PubMed]
11. Wolkoff, P. Indoor air humidity, air quality, and health—An overview. *Int. J. Hyg. Environ. Health* **2018**, *221*, 376–390. [CrossRef] [PubMed]
12. Fang, L.; Clausen, G.; Fanger, P.O. Impact of temperature and humidity on the perception of indoor air quality. *Indoor Air* **1998**, *8*, 80–90. [CrossRef]
13. Posani, M.; Veiga, M.D.R.; de Freitas, V.P. Towards resilience and sustainability for historic buildings: A review of Envelope retrofit possibilities and a discussion on hygric compatibility of thermal insulations. *Int. J. Arch. Herit.* **2019**, *15*, 807–823. [CrossRef]
14. McGregor, F.; Heath, A.; Shea, A.; Lawrence, M. The moisture buffering capacity of unfired clay masonry. *Build. Environ.* **2014**, *82*, 599–607. [CrossRef]
15. Zhang, M.; Qin, M.; Rode, C.; Chen, Z. Moisture buffering phenomenon and its impact on building energy consumption. *Appl. Therm. Eng.* **2017**, *124*, 337–345. [CrossRef]
16. Sesana, E.; Gagnon, A.S.; Bertolin, C.; Hughes, J. Adapting cultural heritage to climate change risks: Perspectives of cultural heritage experts in Europe. *Geosciences* **2018**, *8*, 305. [CrossRef]
17. Posani, M.; Veiga, M.D.R.; De Freitas, V.P.; Kompatscher, K.; Schellen, H. Dynamic hygrothermal models for monumental, historic buildings with HVAC systems: Complexity shown through a case study. *E3S Web Conf.* **2020**, *172*, 15007. [CrossRef]
18. Veiga, M.D.R.; Fragata, A.; Velosa, A.; Magalhães, A.C.; Margalha, G. Lime-based mortars: Viability for use as substitution renders in historical buildings. *Int. J. Arch. Heritage* **2010**, *4*, 177–195. [CrossRef]
19. Ranesi, A.; Veiga, M.R.; Faria, P. Plasters for rehabilitation—Relevant requirements and characteristics. In *4º Encontro de Conservação e Reabilitação de Edifícios—ENCORE*; LNEC—Laboratório Nacional de Engenharia Civil: Lisbon, Portugal, 2020; p. 551. (In Portuguese) [CrossRef]
20. EMB01, Clay Plaster Embarro Universal Technical Sheet. Available online: <https://www.embarro.com/wp-content/uploads/1-CLAY-PLASTER-EMBARRO-UNIVERSAL.pdf> (accessed on 1 February 2020).
21. Freire, M.T. Restoration of Ancient Portuguese Interior Plaster Coatings: Characterization and Development of Compatible Gypsum-Based Products. Ph.D. Thesis, Instituto Superior Técnico, Universidade de Lisboa, Lisbon, Portugal, 2016.
22. Santos, A.R. The Influence of Natural Aggregates on the Performance of Replacement Mortars for Ancient Buildings: The Effects of Mineralogy, Grading and Shape. Ph.D. Thesis, Instituto Superior Técnico, Universidade de Lisboa, Lisbon, Portugal, 2019.
23. Pederneiras, C.M.; Veiga, R.; De Brito, J. Rendering mortars reinforced with natural sheep’s wool fibers. *Materials* **2019**, *12*, 3648. [CrossRef]
24. Farinha, C.B.; de Brito, J.; Veiga, R. Assessment of glass fibre reinforced polymer waste reuse as filler in mortars. *J. Clean. Prod.* **2018**, *210*, 1579–1594. [CrossRef]
25. *Earth Plasters—Requirements, Test and Labelling*; DIN 18947; German Institute for Standardization: Berlin, Germany, 2018.
26. *Gypsum Binders and Gypsum Plasters—Part 2: Test Methods*; EN 13279-2; European Committee for Standardization: Brussels, Belgium, 2004; replaced in 2014.
27. *Methods of Test for Mortar for Masonry—Part 3: Determination of Consistence of Fresh Mortar (by Flow Table)*; EN 1015-3; European Committee for Standardization: Brussels, Belgium, 1999.

28. Pederneiras, C.M.; Veiga, R.; de Brito, J. Physical and mechanical performance of coir fiber-reinforced rendering mortars. *Materials* **2021**, *14*, 823. [\[CrossRef\]](#)
29. *Methods of Test for Mortar for Masonry—Part 6: Determination of Bulk Density of Fresh Mortar*; EN 1015-6; European Committee for Standardization: Brussels, Belgium, 1998.
30. *Methods of Test for Mortar for Masonry—Part 11: Determination of Flexural and Compressive Strength of Hardened Mortar*; EN 1015-11; European Committee for Standardization: Brussels, Belgium, 1999.
31. *Methods of Test for Mortar for Masonry—Part 10: Determination of Dry Bulk Density of Hardened Mortar*; EN 1015-10; European Committee for Standardization: Brussels, Belgium, 1999.
32. *Natural Stone Test Methods—Determination of the Dynamic Modulus of Elasticity (by Measuring the Fundamental Resonance Frequency)*; EN 14146; European Committee for Standardization: Brussels, Belgium, 2004.
33. *Natural Stone Test Method—Determination of Real Density and Apparent Density, and of Total and Open Porosity*; EN 1936; European Committee for Standardization: Brussels, Belgium, 2006.
34. *Methods of Test for Mortar for Masonry—Part 18: Determination of Water Absorption Coefficient Due to Capillary Action of Hardened Mortars*; EN 1015-18; European Committee for Standardization: Brussels, Belgium, 2002.
35. *Conservation of Cultural Property—Test Methods—Determination of Water Absorption by Capillarity*; EN 15801; European Committee for Standardization: Brussels, Belgium, 2009.
36. *Hygrothermal Performance of Building Materials and Products—Determination of Water Vapour Transmission Properties—Cup Method*; ISO 12572; International Organization for Standardization: Geneva, Switzerland, 2016.
37. *Hygrothermal Performance of Building Materials and Products—Determination of Hygroscopic Sorption Properties*; ISO 12571; International Organization for Standardization: Geneva, Switzerland, 2013.
38. Lima, J.; Faria, P.; Silva, A.S. Earth plasters: The influence of clay mineralogy in the plasters' properties. *Int. J. Arch. Heritage* **2020**, *14*, 948–963. [\[CrossRef\]](#)
39. Pavlíková, M.; Kapicová, A.; Pivák, A.; Záleská, M.; Lojka, M.; Jankovský, O.; Pavlík, Z. Zeolite lightweight repair renders: Effect of binder type on properties and salt crystallization resistance. *Materials* **2021**, *14*, 3760. [\[CrossRef\]](#)
40. Černý, R.; Kunca, A.; Tydlitát, V.; Drchalová, J.; Rovnanikova, P. Effect of pozzolanic admixtures on mechanical, thermal and hygric properties of lime plasters. *Constr. Build. Mater.* **2006**, *20*, 849–857. [\[CrossRef\]](#)
41. Mazhoud, B.; Collet, F.; Pretot, S.; Chamoin, J. Hygric and thermal properties of hemp-lime plasters. *Build. Environ.* **2016**, *96*, 206–216. [\[CrossRef\]](#)
42. Cascione, V.; Maskell, D.; Shea, A.; Walker, P.; Mani, M. Comparison of moisture buffering properties of plasters in full scale simulations and laboratory testing. *Constr. Build. Mater.* **2020**, *252*, 119033. [\[CrossRef\]](#)
43. Liuzzi, S.; Rubino, C.; Stefanizzi, P.; Petrella, A.; Boghetich, A.; Casavola, C.; Pappaletta, G. Hygrothermal properties of clayey plasters with olive fibers. *Constr. Build. Mater.* **2018**, *158*, 24–32. [\[CrossRef\]](#)
44. McGregor, F.; Fabbri, A.; Ferreira, J.; Simões, T.; Faria, P.; Morel, J.-C. Procedure to determine the impact of the surface film resistance on the hygric properties of composite clay/fibre plasters. *Mater. Struct.* **2017**, *50*, 193. [\[CrossRef\]](#)
45. Cachová, M.; Vejmelková, E.; Koňáková, D.; Keppert, M. Influence of finely ground brick on hydric properties of lime plasters. In Proceedings of the 4th European Conference of Mechanical Engineering, Paris, France, 29–31 October 2013; pp. 117–121.
46. Vejmelková, E.; Koňáková, D.; Čáchová, M.; Keppert, M.; Černý, R. Effect of hydrophobization on the properties of lime–metakaolin plasters. *Constr. Build. Mater.* **2012**, *37*, 556–561. [\[CrossRef\]](#)
47. Vejmelková, E.; Keppert, M.; Kersner, Z.; Rovnanikova, P.; Černý, R. Mechanical, fracture-mechanical, hydric, thermal, and durability properties of lime–metakaolin plasters for renovation of historical buildings. *Constr. Build. Mater.* **2012**, *31*, 22–28. [\[CrossRef\]](#)
48. Buratti, C.; Belloni, E.; Merli, F. Water vapour permeability of innovative building materials from different waste. *Mater. Lett.* **2020**, *265*, 127459. [\[CrossRef\]](#)
49. Giosuè, C.; Pierpaoli, M.; Mobili, A.; Ruello, M.L.; Tittarelli, F. Influence of binders and lightweight aggregates on the properties of cementitious mortars: From traditional requirements to indoor air quality improvement. *Materials* **2017**, *10*, 978. [\[CrossRef\]](#)
50. Frattolillo, A.; Giovinco, G.; Mascolo, M.; Vitale, A. Effects of hydrophobic treatment on thermophysical properties of lightweight mortars. *Exp. Therm. Fluid Sci.* **2005**, *29*, 733–741. [\[CrossRef\]](#)
51. *Methods of Test for Mortar for Masonry—Part 19: Determination of Water Vapour Permeability of Hardened Rendering and Plastering Mortars*; EN 1015-19; European Committee for Standardization: Brussels, Belgium, 1998.
52. Santos, T.; Gomes, M.I.; Silva, A.S.; Ferraz, E.; Faria, P. Comparison of mineralogical, mechanical and hygroscopic characteristic of earthen, gypsum and cement-based plasters. *Constr. Build. Mater.* **2020**, *254*, 119222. [\[CrossRef\]](#)
53. Santos, T.; Silva, V.; Faria, P. Earthen Mortars—Hygrothermal Behaviour as a Function of Grain Size Distribution of Sand. *Construção Mag.* **2015**, *68*, 28–30. (In Portuguese)
54. Santos, T.; Faria, P.; Silva, V. Characterization of premixed earth mortars. In Proceedings of the Argmassas 2014—Simpósio de Argamassas e Soluções Térmicas de Revestimento, Coimbra, Portugal, 5–6 June 2014; ITeCons: Coimbra, Portugal, 2014; pp. 1–12. (In Portuguese)
55. Jiang, Y.; Phelipot-Mardele, A.; Collet, F.; Lanos, C.; Lemke, M.; Ansell, M.; Hussain, A.; Lawrence, M. Moisture buffer, fire resistance and insulation potential of novel bio-clay plaster. *Constr. Build. Mater.* **2020**, *244*, 118353. [\[CrossRef\]](#)

56. Lima, J.; Faria, P. Eco-efficient earthen plasters: The influence of the addition of natural fibers. In *Natural Fibres: Advances in Science and Technology Towards Industrial Applications. From Science to Markets*; Figueiro, R., Rana, S., Eds.; RILEM Bookseries; Springer: Dordrecht, The Netherlands, 2016; Volume 12, pp. 315–327.
57. Maddison, M.; Muring, T.; Kirsimäe, K.; Mander, U. The humidity buffer capacity of clay-sand plaster filled with phytomass from treatment wetlands. *Build. Environ.* **2009**, *44*, 1864–1868. [[CrossRef](#)]
58. Lima, J.; Faria, P.; Silva, A.S. Earthen plasters based on illitic soils from barrocal region of algarve: Contributions for building performance and sustainability. *Key Eng. Mater.* **2016**, *678*, 64–77. [[CrossRef](#)]
59. Lima, J.; Correia, D.; Faria, P. Earthen plasters: The influence of the addition of gypsum and of the grain size distribution of sand. In Proceedings of the ARGAMASSAS 2016—II Simpósio de Argamassas e Soluções Térmicas de Revestimento, Coimbra, Portugal, 16–17 June 2016; ITeCons: Coimbra, Portugal, 2016; pp. 119–130. (In Portuguese)
60. López-Arce, P.; Gómez-Villalba, L.; Martínez-Ramírez, S.; de Buergo, M.; Fort, R. Influence of relative humidity on the carbonation of calcium hydroxide nanoparticles and the formation of calcium carbonate polymorphs. *Powder Technol.* **2011**, *205*, 263–269. [[CrossRef](#)]
61. Roels, S.; Janssen, H. Is the moisture buffer value a reliable material property to characterise the hygric buffering capacities of building materials? Working paper A41-T2-B-05-7 for IEA Annex 41 project. In *Whole Building Heat Air and Moisture Response*; EBC: Birmingham, UK, 2005.
62. Thomson, M.L.; Lindqvist, J.-E.; Elsen, J.; Groot, C.J.W.P. Porosity of historic mortars. In Proceedings of the 13th International Brick and Block Masonry Conference, Amsterdam, The Netherlands, 4–7 July 2004.
63. Freire, M.T.; Veiga, M.D.R.; Silva, A.S.; de Brito, J. Restoration of ancient gypsum-based plasters: Design of compatible materials. *Cem. Concr. Compos.* **2021**, *120*, 104014. [[CrossRef](#)]
64. Santos, T.; Faria, P.; Silva, V. Can an earth plaster be efficient when applied on different masonries? *J. Build. Eng.* **2019**, *23*, 314–323. [[CrossRef](#)]